European Journal of Applied Physiology
https://doi.org/10.1007/s00421-023-05169-5

ORIGINAL ARTICLE

Modification of the locomotor pattern when deviating from the characteristic heel-to-toe rolling pattern during walking

Raphael M. Mesquita[1] · Giovanna Catavitello[1] · Patrick A. Willems[1] · Arthur H. Dewolf[1]

Received: 30 August 2022 / Accepted: 27 February 2023

Abstract

Purpose Humans are amongst few animals that step first on the heel, and then roll on the ball of the foot and toes. While this heel-to-toe rolling pattern has been shown to render an energetic advantage during walking, the effect of different foot contact strategies, on the neuromuscular control of adult walking gaits has received less attention. We hypothesised that deviating from heel-to-toe rolling pattern affects the energy transduction and weight acceptance and re-propulsive phases in gait along with the modification of spinal motor activity.

Methods Ten subjects walked on a treadmill normally, then placed their feet flat on the ground at each step and finally walked on the balls of the feet.

Results Our results show that when participants deviate from heel-to-toe rolling pattern strategy, the mechanical work increases on average 85% higher ($F = 15.5$; $p < 0.001$), mainly linked to a lack of propulsion at late stance. This modification of the mechanical power is related to a differential involvement of lumbar and sacral segment activation. Particularly, the delay between the major bursts of activation is on average 65% smaller, as compared to normal walking ($F = 43.2$; $p < 0.001$).

Conclusion Similar results are observable in walking plantigrade animals, but also at the onset of independent stepping in toddlers, where the heel-to-toe rolling pattern is not yet established. These indications seem to bring arguments to the fact that the rolling of the foot during human locomotion has evolved to optimise gait, following selective pressures from the evolution of bipedal posture.

Keywords Neuromechanics of walking · Spinal maps · Pendulum-like mechanics · Human locomotion

Introduction

In comparison with other plantigrades (Preuschoft 1970; Gebo 1992; Schmitt and Larson 1995), humans use a heel-to-toe rolling pattern during walking. Indeed, the heel touches the ground first, then the sole rolls from the back to the ball of the foot and toes. Cunningham et al. (2010) hypothesised that during the transition to bipedalism, the foot morphology slowly evolved to a heel-to-toe rolling pattern to facilitate a more economical gait. Indeed, various studies have focussed on the type locomotion of our ancestor *Australopithecus* and much debate exists as to rather they were able to walk fully upright or if they adopted a "hip bent, knee bent", and thus a more flatfoot, walking posture (Kuliukas et al. 2009; Foster et al. 2013). Amongst other reasons for discussion, the former appears to be in accordance with anatomical findings on the vertebral column (Lovejoy and McCollum 2010) and a less energy demanding gait (Crompton et al. 1998) whereas the other descriptions of Lucy's gait is characterised as a "hip bent, knee bent" gait (Stern Jr. and Susman 1983) offering less energetic costs as compared to a quadrupedal gait although higher than an upright gait. The foot morphology of the genus *Homo* evolved to generate lower joint torques during bipedal walking than non-human apes (Holowka and Lieberman 2018). It is therefore well suited for normal human walking (Wang et al. 2014).

From a mechanical point of view, the heel-to-toe rolling pattern modifies the "effective limb length" (*i.e.* hip height) during stance by extending the pivot point of the inverted pendulum—described by the centre of mass of the

Communicated by Jean - Rene Lacour.

✉ Arthur H. Dewolf
arthur.dewolf@uclouvain.be

[1] Laboratoire de Physiologie et Biomécanique de La Locomotion, IoNS Université Catholique de Louvain, 1348 Louvain-La-Neuve, Belgium

Published online: 04 March 2023

body (COM) trajectory (Dewolf et al. 2017)—below the level of the ground (Pontzer 2007; Webber and Raichlen 2016). Also, the translation of the centre of pressure from the heel to the toes (Donelan et al. 2002; Adamczyk et al. 2006; Adamczyk and Kuo 2013) reduces the cost of locomotion by reducing the collisional redirections of the COM and allowing the hip to follow a flatter trajectory (Cunningham et al. 2010; Usherwood et al. 2012). Whereas the comparison between the heel-to-toe rolling pattern and less conventional walking patterns, such as walking on the balls of the feet (Cunningham et al. 2010) or flat-foot walking (Kuliukas et al. 2009; Foster et al. 2013) have been well documented and shows an increase in the energetic cost of locomotion and in the 'external work' done by the COM against the environment (W_{COM}). The consequence of the heel-to-toe rolling pattern on the neuromuscular control of gait is, however, still unclear.

During the course of evolution, motor circuits in the spinal cord were assembled to meet specific body movement requirements and biomechanical functions of limb muscles (Jessell et al. 2011). Progressively, the sequential trunk muscle activation required for undulatory propagation (De Sèze et al. 2008) evolved into more complex and discrete bursts of limb motor-neuronal (MN) activity related to specific kinematic and kinetic events (Lacquaniti et al. 2012) required in bipedal locomotion. For example, in human walking, the estimated alpha-motoneuron (MN) pool activations along the spinal cord fluctuates with the body's centre-of-mass motion, where bursts of activity are visible around the foot-strike and lift-off. In recent years, there has been growing interest in understanding the functional organisation of the spinal locomotor output in the context of its adaptation to different biomechanical requirements (Ivanenko et al. 2008; Chvatal and Ting 2013; Allen and Franz 2018; Dewolf et al. 2020b, 2021a). In particular, biomechanical mechanisms of locomotion, such as the inverted pendulum walking dynamics, are related to a specific spatiotemporal organisation of motor pool activity in the spinal cord (Cappellini et al. 2010; Dewolf et al. 2019).

To further investigate the relationship between the MN activity organisation and biomechanical functions, we examine here how an imposed deviation from the heel-to-toe rolling pattern affects the spatiotemporal dynamics of motor pool activity. To do this, we first asked the subjects to walk on the balls of their feet (low-digitigrade condition) then to keep the foot flat on the ground (flat-foot condition) and finally, compared this to normal walking. In particular, we compared the fluctuation of energy of the COM, the lower-limb kinematics and the spinal motor output in each condition. Based on previous published findings presented here above, we hypothesised that deviating from the heel-to-toe rolling pattern would (1) modify the actively regulated exchange in energy during walking since the weight acceptance and re-propulsion phases are adjusted and (2) increase the directional change of the COM during the step-to-step transition. Consequently, the neuromuscular control of gait will be affected. This latter change will be highlighted by increased motor unit burst durations and smaller intervals between lumbar and sacral co-activations.

Methods

Subjects

Six males and four females (age: 22.2 ± 2.4 y, mass: 69.2 ± 14.4 kg, height: 1.75 ± 0.10 m, mean ± SD) volunteered to participate in this study. All of the participants provided informed consent and the procedures used for this study were approved by the ethics committee of the Université catholique de Louvain (Ref. No. 2015/06JUL/372) and were performed according to the Declaration of Helsinki.

Experimental procedure and data collection

Subjects were asked to walk wearing their own walking shoes on an instrumented treadmill at 1.11 m s^{-1} (4 km h^{-1}), *i.e.* a comfortable walking speed close to the most economical normal walking speed based on the net energy consumption (Cavagna and Kaneko 1977). Three different types of walking were tested: first, a trial using the natural foot contact (called 'normal walking condition', NW), second, the subjects were instructed to place the foot flat on the ground with the knees bent (called 'flat-foot plantigrade walking condition', FP), third, they were instructed to walk on tiptoes (*i.e.* on the distal metatarsal heads) and to keep the heel slightly elevated above the ground during stance (called 'low-digitigrade walking condition', LD). These gaits were demonstrated to the subjects after a verbal explanation. Before starting the data collection, participants had the opportunity to carry out several tries with oral feedback from the experimenter. For each trial, data collection lasted 30 s and on average, 26.8 ± 2.2 (mean ± SD) strides were recorded.

Four force transducers (Arsalis, Belgium) were placed under the body of an instrumented treadmill with a belt surface of 1.6 × 0.65 m (Stellar—H/P/ Cosmos, Germany). They measured the vertical (F_v), the forward (F_f) and the lateral (F_l) components of the force (GRF) exerted by the feet on the tread-belt, as in Dewolf et al. (2017). Twelve reflective markers were glued on the following anatomical landmarks on the right side of the body: the chin-neck intersect (C2), the greater trochanter (GT), at mid-distance along the middle of the lateral side of the thigh (IT), the external femoral condyle (CE), the external malleolus (ME) and the fifth metatarsophalangeal joint (MT5). The position of each

marker in the sagittal plane was measured by means of a high-speed video camera (BASLER A501k, sampling rate 100fps), placed perpendicularly to the plane of progression. The coordinates of the landmarks in the fore-aft and vertical directions were tracked each frame using a custom-made LabVIEW software, as in Mauroy et al. 2014; Dewolf and De Jaeger 2015 and in Dewolf et al. 2018.

Electromyographic (EMG) activities from 16 muscles on the right side of the subject were recorded at 2 kHz using a Delsys Trigno Wireless System (Boston, MA): erector spinae (ES) at L2 level, gluteus maximus (Gm), gluteus medius (Gmed), sartorius (SART), tensor fasciae latae (TFL), adductor longus (ADD), vastus medialis (VM), vastus lateralis (VL), rectus femoris (RF), biceps femoris long head (BF), semitendinosus (ST), tibialis anterior (TA), medial gastrocnemius (MG), lateral gastrocnemius (LG), soleus (SOL) and peroneus longus (PERL). After shaving, the skin was rubbed with fine sandpaper, ether and alcohol and EMG electrodes were placed based on suggestions from SENIAM (the European project on surface EMG—seniam.org). To ensure correct placement of EMG electrodes, muscle bellies were located by means of palpation and the electrodes were oriented along the main direction of the fibres (Kendall et al 2005). We verified electrode position and signal quality by visually inspecting the EMG signals while subjects contracted each instrumented muscle. Acquisitions of the EMG, kinematic, and kinetic data were synchronised by means of an external 5 V TTL trigger signal.

Data analysis

Division of the stride: the stride period was defined as the time between two successive right foot contacts (FC). FC and toe off (TO) were estimated from the displacement of the centre of pressure (COP) on the belt (Meurisse et al. 2016).

Kinetics: The acceleration, velocity, displacement of the COM and the external energy (E_{COM}) and power (P_{COM}) were evaluated from the GRF using the procedure described in detail in Dewolf et al. (2017) and described only briefly here. The fore-aft, lateral and vertical acceleration of the COM were respectively computed as $a_f = F_f/m$, $a_l = F_l/m$ and $a_v = (F_v\text{-}m\,g)/m$, where m is the subject's body mass and g is the acceleration of gravity. The instantaneous velocity in the fore-aft, lateral and vertical directions were obtained by integration of a_f, a_l and a_v plus an integration constant. In the fore-aft direction, this constant was chosen to make the average velocity over the stride equal to the velocity of the tread-belt, measured with an optical encoder. In the two other directions, constants were chosen to make the average vertical and lateral velocity over each stride equal to zero. A second integration of the vertical velocity yields the vertical displacement of the COM.

E_{COM}, the energy of the COM was computed as the algebraic sum at each instant of its gravitational potential energy E_p and of its kinetic energy E_k. The work W_{COM} represents the work necessary to move the COM relative to the surroundings. Positive (W^+_{COM}) and negative (W^-_{COM}) were computed by summing the increments and the absolute value of the decrements the E_{COM}-time curve, respectively (Cavagna et al. 1976; Dewolf et al. 2016). Similarly, W^+_k,W^-_k, W^+_p and W^-_p were computed by summing respectively the increments and the absolute value of the decrements of the E_k and E_p curves. Due to the out-of-phase oscillation of E_p and E_k occurring during walking, energy is recovered by transduction between potential and kinetic energy, and vice versa. The periods during which an E_p-E_k transduction occurred was determined by measuring the recovery at each instant t of the step, $r(t)$, using following equation (Cavagna et al. 2002; Dewolf et al. 2017):

$$r(t) = 100\,\frac{\left|E_k(t)-E_k(t-\Delta t)\right| + \left|E_p(t)-E_p(t-\Delta t)\right| - \left|E_{ext}(t)-E_{ext}(t-\Delta t)\right|}{\left|E_k(t)-E_k(t-\Delta t)\right| + \left|E_p(t)-E_p(t-\Delta t)\right|},$$

where Δt is the time between two samples. The %-recovery was defined as the average r(t) across a stride. Two periods of energy transduction (T1 and T3) occurred during a step: T1 when E_p increases while E_k decreases and T3 when E_p decreases while E_k increases (Dewolf et al. 2017). The mechanical power, $\dot{e}(t)$, recovered by the E_p-E_k transduction, was computed as:

$$\dot{e}(t) = \frac{\left|E_k(t)-E_k(t-\Delta t)\right| + \left|E_p(t)-E_p(t-\Delta t)\right| - \left|E_{ext}(t)-E_{ext}(t-\Delta t)\right|}{\Delta t}$$

The amount of energy recovered (E_s) over a given period was computed by integration of the $\dot{e}(t)$-time curve.

The external power P_{COM} was computed by: $P_{COM} = dE_{COM}/dt$. During a walking stride, the P_{COM}-time curve typically presents one major negative peak ($\dot{W}^-$) and two major of positive peaks, $\dot{W}^+_1$ and $\dot{W}^+_2$, also called weight acceptance and propulsion, respectively (Cavagna et al. 1976; Dewolf et al. 2019). In the present study, the maximum value of each of these peaks were measured across all conditions.

Kinematics: From the marker locations, the orientation of the thigh, shank, foot and trunk segments relative to the vertical axis (elevation angle) were computed as described in Borghese et al. (1996). The joint angles (hip, knee, and ankle) were then computed from the elevation angles of adjacent segments. The range of angular motion (ROM) was computed for each angular waveform by the difference between the maximum and the minimum values over the entire stride and over the stance phase. For each subject, the

different strides of each trial were time-normalised by interpolating individual gait cycles over 200 points (*i.e.,* each point corresponding to 0.5% of the stride).

EMG: The 16 collected raw EMG signals were high-pass filtered (30 Hz), then rectified and low-pass filtered with a zero-lag 4th-order Butterworth filter (10 Hz). A custom-made automatic search for artefacts was also implemented, by comparing the EMG envelope of the gait cycle with the average envelope across all strides. The time scale was normalised by interpolating individual gait cycles over 200 points. For each condition and for each EMG waveform, the full width at half maximum (FWHM) was calculated as the period during which the EMG activity exceeded the half of its maximum (Martino et al. 2014; Santuz et al. 2020). The centre of activity (CoA) of each EMG waveform was also calculated as the angle of the vector that points to the centre of mass of the circular distribution (Martino et al. 2014). The CoA was chosen because it was impractical to reliably identify a single peak of activity in the majority of muscles. It is a qualitative parameter helpful to understand the distribution of muscular activity.

The EMG activities were then mapped onto the estimated rostro-caudal location of the MN pools in the human spinal cord from the L2 to S2 segments based on Kendall's myotomal charts (Kendall et al. 2005), as in Ivanenko et al. (2006). To account for size differences in MN pools at each spinal level, this fractional activity value was then multiplied by the estimated segment-specific number of MNs (MNj), based on Tomlinson and Irving (1977).

To compute the total motor output in each condition, the motor output patterns of each spinal segment over the gait cycle were summed. The minimal activation and the range (the difference between the max and min values) were then computed. The relative activation of the lumbar and sacral segments in each condition were computed as the average motor output patterns in the upper part of the lumbar (sum of the activity from L2 to L4) and the sacral segments (sum of activity from S1 to S2). Note that to reduce overlaps due to map- smoothing, the spinal segment L5 was not taken into account (Dewolf et al. 2019, 2020a). The FWHM and the timing of the maximal activation were then calculated for both lumbar and sacral segments.

Statistics

The statistical analysis was designed to assess the effect of foot–ground interactions. A linear mixed model was applied. The normality of the residuals was checked visually with QQ-plots. Circular statistics (Berens 2009) was used to characterize the CoA of each muscle and spinal output. The Rayleigh test (Berens 2009) was used to check whether the samples were distributed uniformly around the gait cycle or had a common mean direction. In all analyses, the significance level was fixed at $p < 0.05$. Statistical analyses were performed with the statistical software package IBM SPSS (Version 23.0).

Results

General gait parameters and joint angles

Figure 1 presents the average traces of the hip-, knee- and ankle-angles during one cycle with different foot–ground interactions, compared with the normal walking condition (in light grey). The duration of the cycle was affected by foot-placement ($F = 8.6$; $p = 0.001$, Fig. 1B), with a shorter cycle occurring both in LD ($p = 0.002$) and FP ($p = 0.007$) as compared to the heel-to-toe rolling pattern (NW). However, relative duration of contact phase was not affected by walking condition ($F = 0.817$; $p = 0.452$). The hip range of motion (ROM) over the stride was greater during as compared to the other conditions ($p < 0.013$), whereas the knee ROM was smaller both in FP and LD as compared to NW ($p < 0.009$, Fig. 1B). During the stance phase, the hip range of motion was not affected by LD nor by FP ($F = 2.1$; $p = 0.146$), whereas the knee ROM was smaller in LD as compared to NW ($p = 0.008$).

Instead, the ankle ROM over the stride was not affected by the two different conditions ($F = 0.2$; $p = 0.813$). When considered over the stance phase only, the ankle ROM was smaller in FP condition as compared to NW ($p = 0.003$). The major modification in FP was a more flexed hip ($p < 0.001$) and knee ($p < 0.001$) mean position, whereas the major modification during LD was a greater ankle extension ($p = 0.017$).

Mechanical work

Figure 2 illustrates a typical trace of the COM energy and the time course of the instantaneous recovery, r(t), and the rate, $\dot{e}$(t), of pendular energy savings within one stride in each condition. The W_{COM} was significantly different between conditions ($F = 15.5$; $p < 0.001$, Fig. 1B): W^{+}_{COM} was greater both in FP ($p = 0.02$) and in LD than in NW ($p = 0.047$). This greater W_{COM} could be partly explained by the different %recovery over a stride between conditions (Fig. 2B; $p < 0.01$).

The duration of T1 was reduced in FP ($F = 24.0$; $p < 0.001$). During T1, the amount of energy saved through the pendulum-like energy exchange (E_s) was different between conditions ($F = 28.4$; $p < 0.001$), being smaller when deviating from the heel-to-toe rolling pattern. The duration of T3 was also reduced in FP ($F = 21.8$;

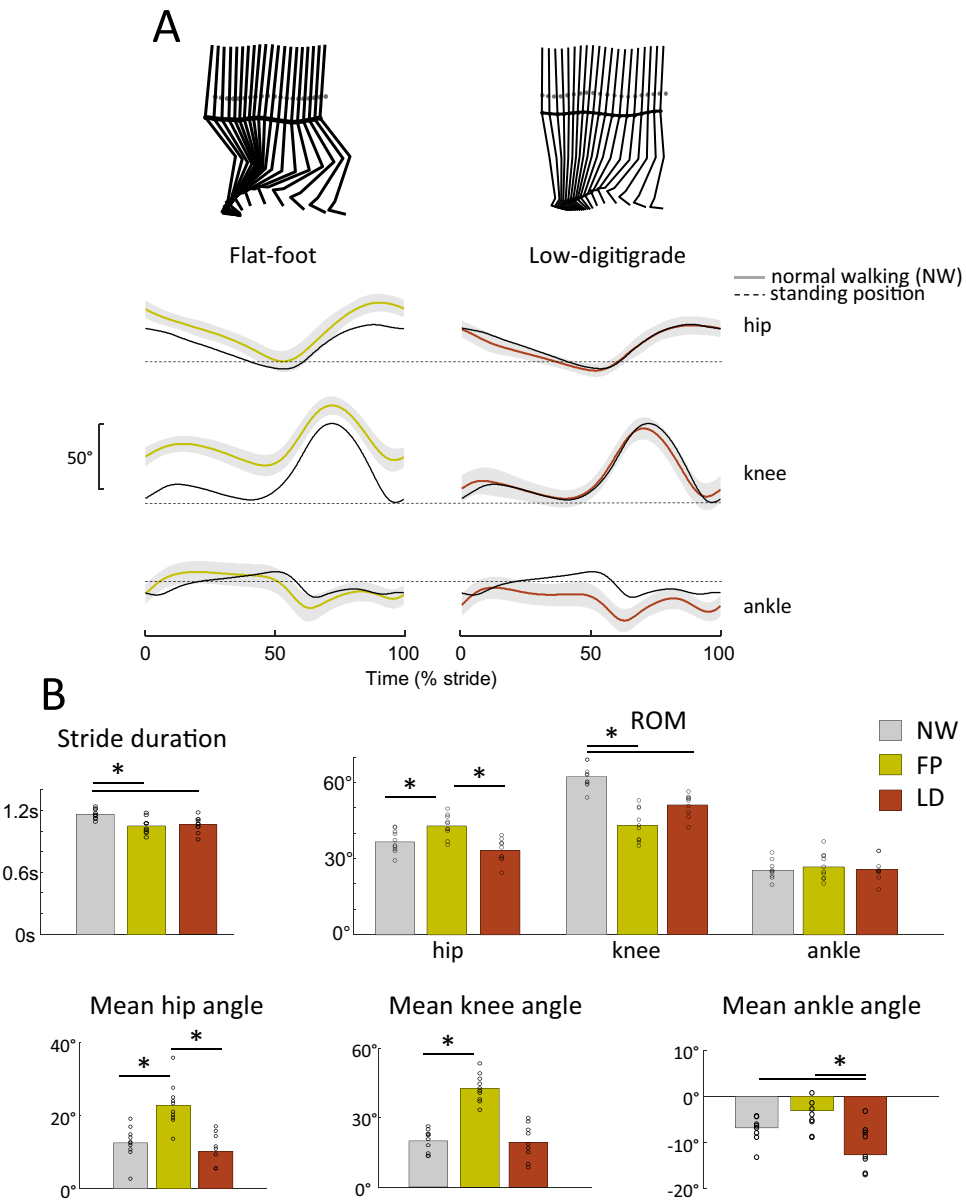

Fig. 1 Kinematics of lower-limb joint angles and general gait parameters during 'normal walking' (NW), 'flat-foot plantigrade' walking (FP) and 'low-digitigrade' walking (LD) **A –** Angles of the hip, knee and ankle over a stride. All the curves of each subject walking at a given walking condition were first averaged (mean-curve). The curves presented here are the average of the mean-curves of all the subjects. The black curves correspond to NW. The grey zone represents ± 1 SD for the FP (green) and LD (red) conditions. The interrupted lines correspond to the standing position. A positive value corresponds to (dorsi-) flexion. In each condition, the stickman at the top illustrates the position of the segments, every 5% of a typical stride of 1 subject. **B** – the bar plots present the average stride duration, the average range of motion of the hip, knee and ankle over one stride and their average angle over one stride. Each dot represents the average across all strides of per subject. In all panels, grey bars correspond to normal walking. Asterisks (*) indicate a significant difference between conditions ($p < 0.05$)

$p < 0.001$). The amount of energy saved during T3 was not affected by any conditions ($F = 2.9$; $p = 0.068$).

The Fig. 3A presents typical vertical ground reaction forces during one stride (2 steps) and the power curves (P_{COM}). Despite the large kinematic differences between the conditions, the vertical GRF- and power curves are rather similar, especially in NW and LD. The peaks of power production were affected by foot–ground interactions (Fig. 3B): $\dot{W}_1^+$ was greater, and the $\dot{W}_2^+$ was smaller in both FP and LD as compared to NW ($\dot{W}_1^+$: $F = 9.3$; $p < 0.01$;$\dot{W}_2^+$: $F = 4.6$; $p = 0.039$). The negative peak of power $\dot{W}^-$ was instead greater in both FP and LD as compared to NW ($F = 12.3$; $p < 0.001$).

Spinal maps

Figure 4 illustrates the ensemble-averages (*i.e.,* across subjects) of rectified EMG envelopes for all walking conditions. Figure 5A presents the EMG signals of Fig. 4 mapped onto the estimated rostro-caudal location of the MN pools in the spinal cord. Both the lumbar and sacral segments presented one major spot of activity (Ivanenko et al. 2006; Cappellini et al. 2010; Dewolf et al. 2019). The lumbar mean intensity increased when deviating from the heel-to-toe rolling pattern ($F = 5.5$; $p = 0.011$), especially during FP. The sacral mean intensity only changes during LD due to tonic activation of ankle extensor during stance as compared to NW

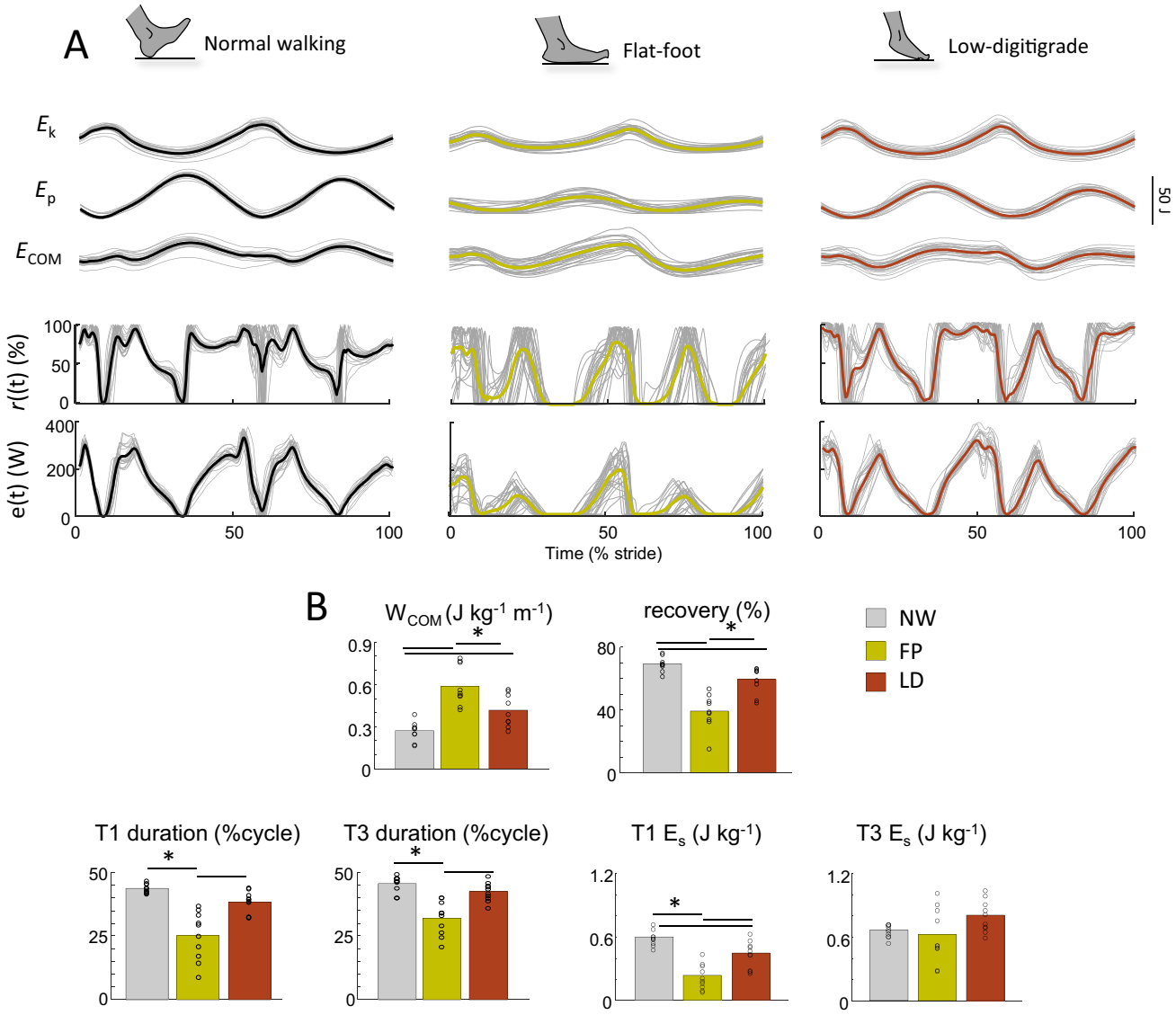

Fig. 2 Centre of mass mechanics in all conditions **A** – Typical time-traces of the mechanical energy-time curves of the COM of one subject walking in the three tested conditions. *Top*: the upper curve (E_k) refers to the kinetic energy of the COM, the middle curve (E_p) to its gravitational potential energy and the bottom curve ($E_{COM} = E_k + E_p$) to the total energy of the COM. *Middle*: instantaneous recovery at each instant t of the stride. The recovery r(t) varies form 0% when the E_k and E_p curves are in phase, to 100% when the decrease of one curve equals the increase of the other. *Bottom:* The rate of pendular energy savings e(t) at each instant t of the stride. These curves represent the rate at which energy is economised through the transformation of kinetic into potential energy (or vice versa). The grey lines correspond to individual strides whereas the coloured thick lines correspond to the average across all strides. **B –** the bar plots present the average positive W_{COM}, the average recovery over one stride, the duration of T1 and T3 and the average amount of energy exchange over those periods. The dots represent the average across all strides of one subject. In all panels, grey bars correspond to normal walking. Asterisks (*) indicate a significant difference between conditions ($p < 0.05$)

($p = 0.02$). No significant differences were observed in the lumbar-sacral co-activation.

Another striking difference was the burst timing and duration of the spinal segments. As compared to NW, the CoA of the lumbar segments occurred later in the stance ($p = 0.02$) and the CoA of the sacral segments occurred earlier in the stance ($p < 0.001$) when deviating from normal foot–ground interaction. As a result, the delay between the lumbar and sacral CoA was smaller in FP and LD than in NW ($F = 43.2$; $p < 0.001$).

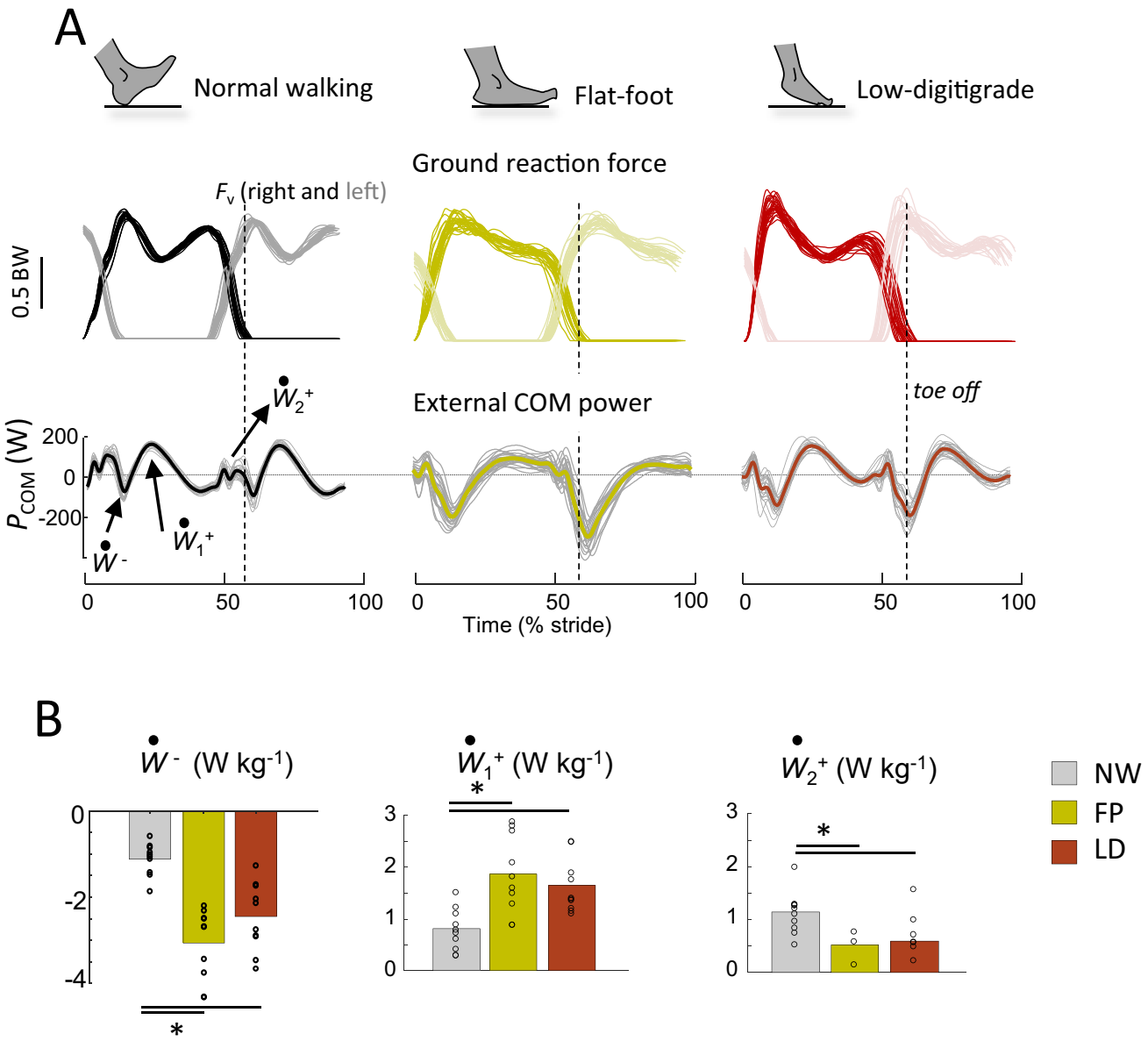

Fig. 3 Characteristics of the Ground Reaction Forces **A – Top:** typical time-traces of the vertical GRF of one subject walking in the three tested conditions. *Middle*: Average time-traces of the external COM power P_{COM} in the three tested conditions. The grey lines correspond to the average across strides for one subject whereas the thick lines are the average across strides. The interrupted vertical lines are the toe off. **B –** Average negative peak of P_{COM} ($\dot{W}^-$, left), and average positive peaks of P_{COM} during weight acceptance ($\dot{W}_1^+$, middle) and during propulsion ($\dot{W}_2^+$, right). Asterisks (*) indicate a significant difference between conditions ($p < 0.05$)

Discussion

In this study, we examined neuromechanical relationships between different foot–ground interactions during walking and the lower-limb muscular activation patterns, the associated spinal motor pool activation, lower-limb joint kinematics and COM kinetics. Despite the rather novel conditions imposed on participants, we observed major differences between the three forms of walking which cannot only be assigned to a lack of practise. When the subjects deviate from the heel-to-toe rolling pattern, the peak propulsion power at the end of stance is reduced, which in turn, implies that there is a greater downward velocity of the COM at foot contact and therefore that a greater peak power at weight acceptance (Fig. 3A). A lack of ankle push-off power has been shown to have compensatory effects on the rest of the stride, leading to a rise in W_{COM} done during the midstance and a redistribution of work across the other lower-limb joints (Huang et al. 2015). Below, we discuss the changes of kinematics and

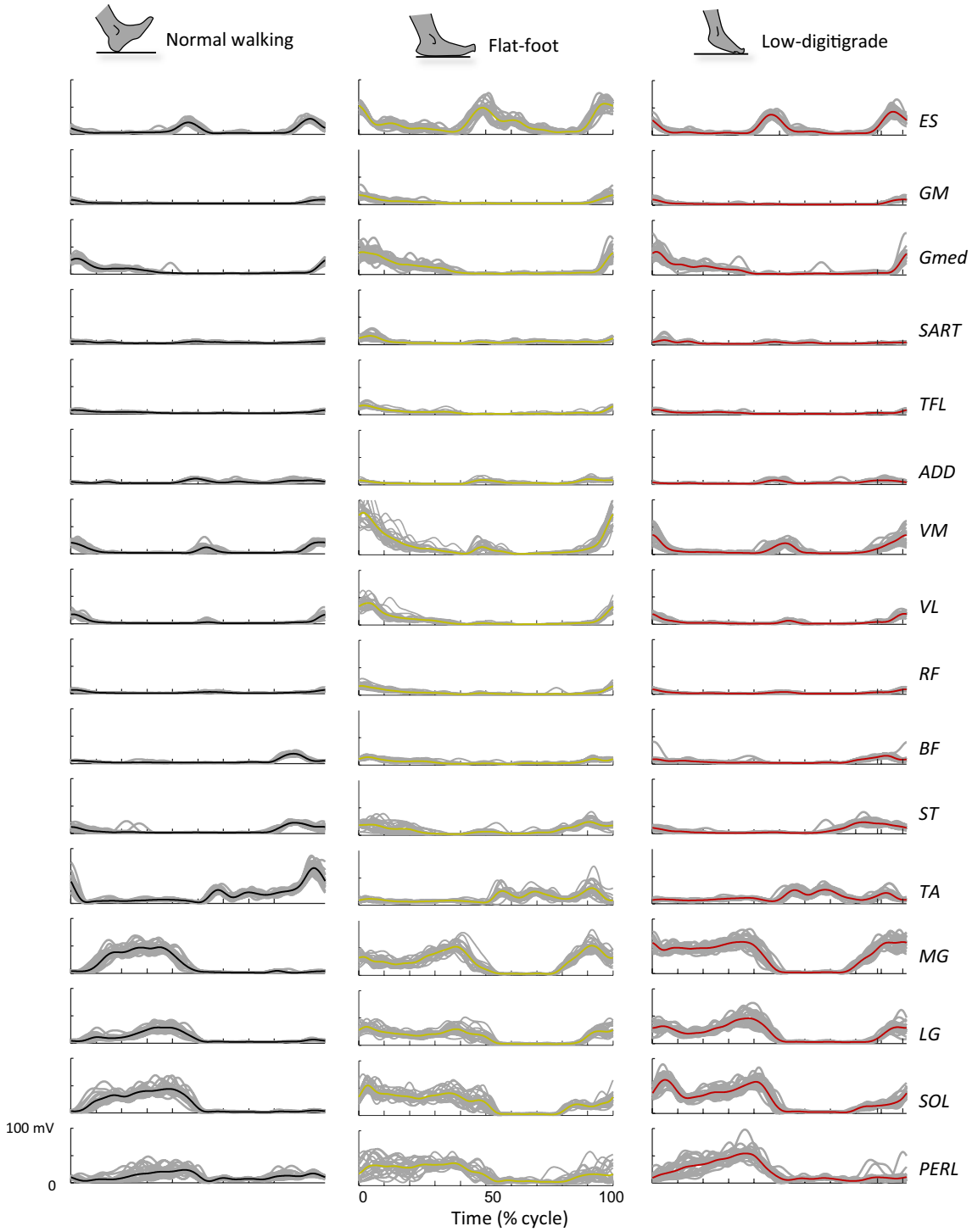

Fig. 4 Ensemble-averaged electromyogram (EMG) patterns during flat-foot, low-digitigrade and normal walking *ES* erector spinae, *GM* gluteus maximus, *Gmed* gluteus medius, *SART* sartorius, *TFL* tensor fascia latae, *ADD* adductor longus, *VM* vastus medialis, *VL* vastus lateralis, *RF* rectus femoris, *BF* biceps femoris, *ST* semitendinous, *TA* tibialis anterior, *MG* gastrocnemius medialis, *LG* lateral gastrocnemius, *SOL* soleus, *PERL* peroneus longus. The thick curves presented here are the average of the mean-curves (grey) of all the subjects

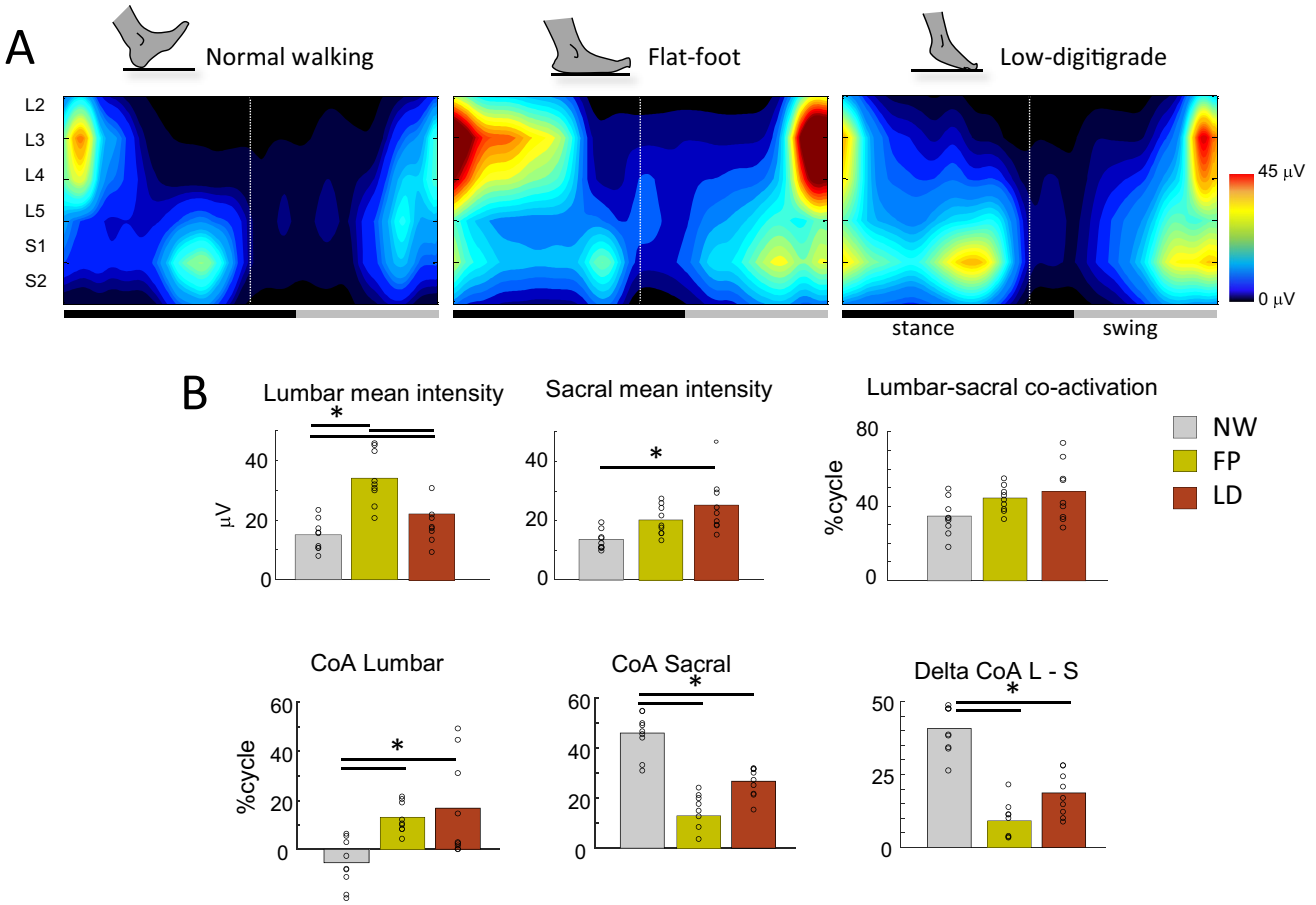

Fig. 5 – Unilateral spatiotemporal spinal motor outputs computed from ensemble-averaged electromyograms (EMGs) across all subjects in all conditions **A –** Motor output (reported in ΔV) is plotted as a function of gait cycle in the three conditions. **B –** the bar plots present the average level of activation of the lumbar and sacral motor output, average lumbar-sacral co-activation, centre of activation (CoA) of the lumbar and sacral segments output and time delay between lumbar and sacral CoA. Asterisks (*) indicate a significant difference between conditions ($p < 0.05$)

segmental spinal motor output in relation to a change in power production.

As observed by Dewolf et al. (2019), the modification of the mechanical requirements at the step-to-step transition reflects changes of the power peaks, inducing a different involvement of both lumbar and sacral segment activation. The reduction of propulsive power generation is related to the imposed reduction of ankle plantarflexion at the end of stance (Fig. 1). Consequently, due to the lack of ankle push-off from the trailing limb, the redirection of the COM velocity occurs after the contact of the leading limb with the ground (Meurisse et al. 2019) as the vertical velocity continues to decrease after heel strike (Fig. 3B). In turn, the weight-acceptance phase increases during the first part of stance after the foot touches the ground (Fig. 3B). This effect is lessened during LD, since the heel-off (not present during flat-foot walking) already contributes slightly to the COM redirection (Hu et al. 2021). Another interesting observation is that the modifications of foot contact strategy results in changes of the timing of lumbar and sacral activations (Fig. 5). During normal walking, the main burst of lumbar activation occurs around ground contact (0%, close to the weight acceptance peak) and the main burst of sacral activation at the end of stance (45%, close to the propulsion peak). Without a heel-to-toe rolling pattern, the CoA of lumbar and sacral segments are closer together.

The present comparison of different human gaits and developmental considerations (Fig. 6) further highlights the link between global biomechanical parameters, such as COM dynamics, and functional spinal cord topography. On the one hand, in neonate stepping, sequential activation of spinal segments and bursts of activity around touchdown and foot lift-off are not yet developed and both lumbar and sacral motor pools are simultaneously activated during midstance (Ivanenko et al. 2013). With the progressive development of the heel-to-toe rolling pattern, the distinction of lumbar and sacral segment activation and the COM mechanism and recovery become closer to the adult values (Fig. 6; Cheron

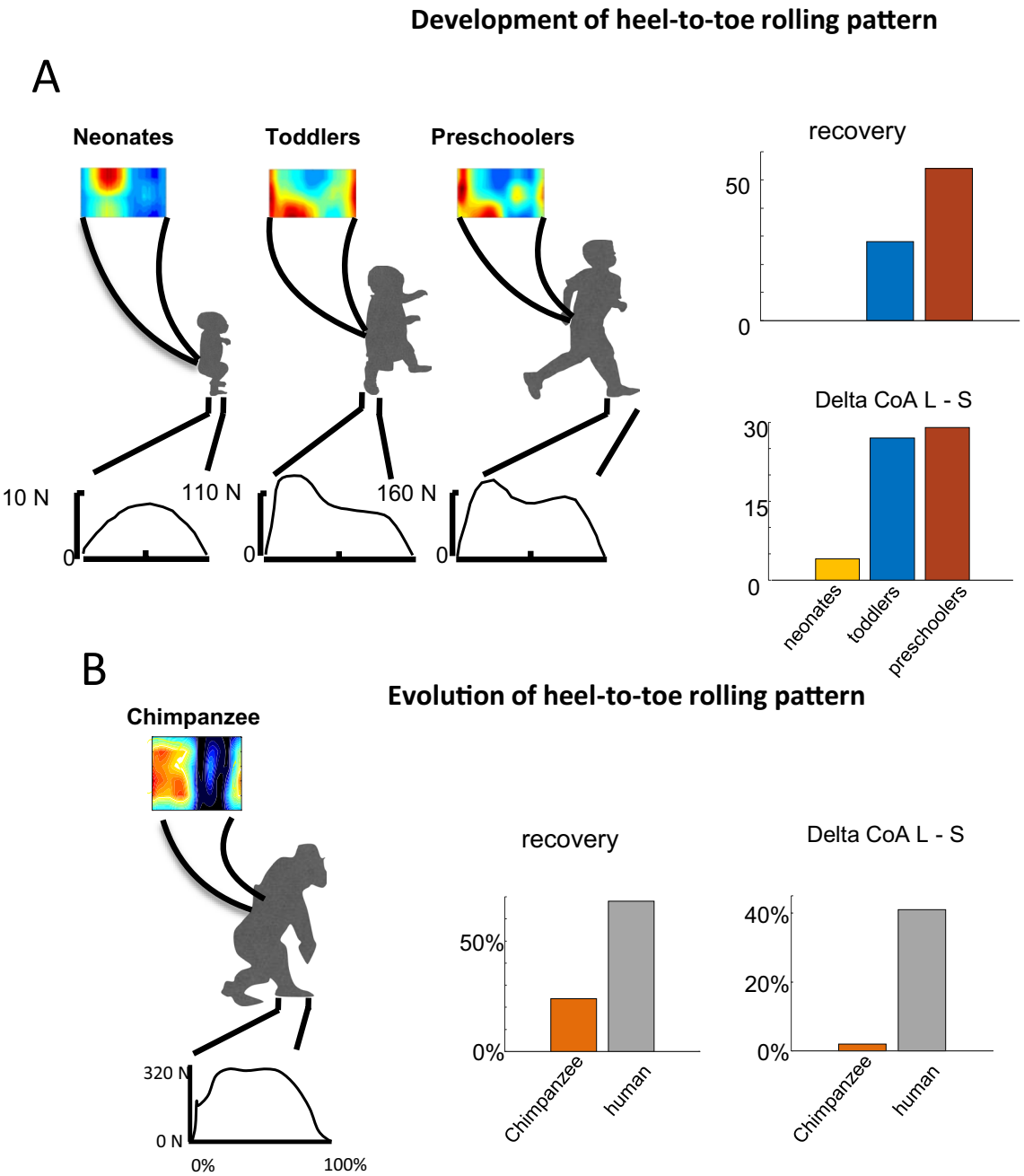

Fig. 6 Development and evolution of the heel-to-toe rolling pattern **A –** Effect of age on the spinal motor output and the vertical ground reaction force (redrawn with permission from (Dewolf et al. 2020c)). On the right, the bar plots present an the recovery and the time delay between lumbar and sacral CoA at different development stage in human (from (Ivanenko et al. 2008, 2013)). **B –**Estimation of the spinal motor output and the vertical ground reaction force (estimated based on the data of Shapiro and Jungers 1994; Demes et al. 2015; Wei et al. 2019; Higurashi et al. 2019) in great apes. On the right, the bar plots present the recovery and the time delay between lumbar and sacral CoA estimated from the reconstructed spinal motor output presented on the left

et al. 2001; Ivanenko et al. 2004; Hallemans et al. 2006; Dewolf et al. 2020c). On the other hand, in older adults, a reduction of ankle push-off is observed at the end of stance, resulting in modified COM mechanics and an earlier activation of the sacral segments (Monaco et al. 2009; La Scaleia et al. 2014; Santuz et al. 2020; Dewolf et al. 2021b, a), making the lumbar and sacral motor pools closely activated during midstance.

Deviation from the heel-to-toe rolling pattern, due to pathologies for example, may involve modifications to the COM mechanics and muscular activity (Cappellini et al. 2016). For example, one major constraint in spastic

cerebral palsy is the less extensible plantar flexors (Barber et al. 2011), that may force patients to walk in an 'equinus gait' (LD-like foot interaction with the ground). Typically, it is associated with less propulsion during gait (Dallmeijer et al. 2011), and a smaller delay between lumbar and sacral segment activation (Cappellini et al. 2020).

Such investigations of spatiotemporal patterns of spinal cord activations in relation with different biomechanical requirements may also have important clinical implications. For instance, a differential spinal cord epidural or transcutaneous stimulation (Angeli et al. 2018; Gill et al. 2018) could potentially result in differential activation of spinal segments to selectively drive neuro-prostheses depending on walking conditions.

In living primates, with the exception of the great apes and humans, the foot is placed in a heel-elevated or semi-plantigrade position when these animals move upon the ground (Gebo 1992). In millions of years of bipedal evolution, the hominid foot underwent notable changes after long evolutionary processes (Hu et al. 2021) and the human heel-to-toe rolling pattern has been adopted. This refinement of the locomotor strategy has been selected to optimise gait, this is potentially highlighted by the result of deviation from the heel-to-toe pattern on the motor pool activation and mechanical demand observations. Indeed, the absence of a heel-to-toe rolling pattern in adults or in great apes results in similar modifications of muscle timing of activation (Shapiro and Jungers 1994; Wei et al. 2019; Higurashi et al. 2019). Also, similar COM mechanics can be observed, with for example a higher mechanical work and smaller recovery for chimpanzee (Demes et al. 2015) (Fig. 6). Therefore, it may suggest that the specific neuromuscular patterns of human gait (*i.e.,* the dissociated lumbar and sacral bursts of activation) have been influenced by the evolutionary changes of foot morphology, for example a longer posterior calcaneus and shorter toes. However, this suggestion should not neglect that these patterns are also adopted through years of locomotion experience (Fig. 6B).

Limitations

There are some limitations to our study that cannot be neglected. The main one is the fact that we are comparing normal walking, performed daily, with a novel gait with which the subjects have no experience, implies that part of the difference observed between gaits could potentially be reduced with appropriate training and that results obtained should take this novelty into account. Furthermore, the trial order was not randomised which can affect the order in which subjects discover each condition along with increased fatiguability.

Conclusion

Our results seem to bring arguments to the fact that the rolling of the foot during human locomotion has evolved to optimise gait, following selective pressures from the evolution of bipedal posture. Over millennia, the heel-to-toe rolling pattern came about to facilitate a more economical gait (Cunningham et al. 2010). Normal walking seems to have adopted the most efficient inverted-pendular mechanism thus producing the least amount of external work by the COM. Furthermore, much like the locomotion in toddlers, without a heel-to-toe rolling pattern, the CoA of lumbar and sacral segments are closer together as the lower limb needs to adapt for increased weight-acceptance peaks after touchdown. With development, as with evolution, the values for CoA, recovery and COM mechanism become those seen in adults today.

Author contributions Conceptualisation: RMM, AHD, GC, PAW. Data curation: PAW Formal analysis: AHD, RMM & GC. Funding acquisition: PAW. Investigation: AHD, RMM, GC & PAW. Methodology: AHD, RMM, GC and PAW. Project administration: AHD. Software: AHD. Supervision: AHD. Writing—original draft: RMM & AHD. Writing—review & editing: RMM, GC, PAW, AHD.

Data availability Data are available upon reasonable request.

Declarations

Conflict of interest The authors declare no conflict of interest.

References

Adamczyk PG, Kuo AD (2013) Mechanical and energetic consequences of rolling foot shape in human walking. J Exp Biol 216:2722–2731. https://doi.org/10.1242/jeb.082347

Adamczyk PG, Collins SH, Kuo AD (2006) The advantages of a rolling foot in human walking. J Exp Biol 209:3953–3963. https://doi.org/10.1242/jeb.02455

Allen JL, Franz JR (2018) The motor repertoire of older adult fallers may constrain their response to balance perturbations. J Neurophysiol 120:2368–2378. https://doi.org/10.1152/jn.00302.2018

Angeli CA, Boakye M, Morton RA et al (2018) Recovery of overground walking after chronic motor complete spinal cord injury. N Engl J Med 379:1244–1250. https://doi.org/10.1056/NEJMoa1803588

Barber L, Barrett R, Lichtwark G (2011) Passive muscle mechanical properties of the medial gastrocnemius in young adults with spastic cerebral palsy. J Biomech 44:2496–2500. https://doi.org/10.1016/j.jbiomech.2011.06.008

Berens P (2009) CircStat: A MATLAB toolbox for circular statistics. J Stat Softw 31:1–21

Borghese NA, Bianchi L, Lacquaniti F (1996) Kinematic determinants of human locomotion. J Physiol 494:863–879

Cappellini G, Ivanenko YP, Dominici N et al (2010) Migration of motor pool activity in the spinal cord reflects body mechanics in human locomotion. J Neurophysiol 104:3064–3073

Cappellini G, Ivanenko YP, Martino G et al (2016) Immature spinal locomotor output in children with cerebral palsy. Front Physiol. https://doi.org/10.3389/fphys.2016.00478

Cappellini G, Sylos-Labini F, Dewolf AH et al (2020) Maturation of the locomotor circuitry in children with cerebral palsy. Front Bioeng Biotechnol 8:998. https://doi.org/10.3389/fbioe.2020.00998

Cavagna GA, Kaneko M (1977) Mechanical work and efficiency in level walking and running. J Physiol 268:467–481. https://doi.org/10.1113/jphysiol.1977.sp011866

Cavagna GA, Thys H, Zamboni A (1976) The sources of external work in level walking and running. J Physiol (lond) 262:639–657. https://doi.org/10.1113/jphysiol.1976.sp011613

Cavagna GA, Willems PA, Legramandi MA, Heglund NC (2002) Pendular energy transduction within the step in human walking. J Exp Biol 205:3413–3422

Cheron G, Bouillot E, Dan B et al (2001) Development of a kinematic coordination pattern in toddler locomotion: planar covariation. Exp Brain Res 137:455–466

Chvatal SA, Ting LH (2013) Common muscle synergies for balance and walking. Front Comput Neurosci 7:48. https://doi.org/10.3389/fncom.2013.00048

Crompton RH, Weijie LYW, Günther M, Savage R (1998) The mechanical effectiveness of erect and "bent-hip, bent-knee" bipedal walking in Australopithecus afarensis. J Hum Evol 35:55–74. https://doi.org/10.1006/jhev.1998.0222

Cunningham CB, Schilling N, Anders C, Carrier DR (2010) The influence of foot posture on the cost of transport in humans. J Exp Biol 213:790–797. https://doi.org/10.1242/jeb.038984

Dallmeijer AJ, Baker R, Dodd KJ, Taylor NF (2011) Association between isometric muscle strength and gait joint kinetics in adolescents and young adults with cerebral palsy. Gait Posture 33:326–332. https://doi.org/10.1016/j.gaitpost.2010.10.092

De Sèze M, Falgairolle M, Viel S et al (2008) Sequential activation of axial muscles during different forms of rhythmic behavior in man. Exp Brain Res 185:237–247. https://doi.org/10.1007/s00221-007-1146-2

Demes B, Thompson NE, O'Neill MC, Umberger BR (2015) Center of mass mechanics of chimpanzee bipedal walking. Am J Phys Anthropol 156:422–433. https://doi.org/10.1002/ajpa.22667

Dewolf A, De Jaeger D (2015) Effect of stride length on maximal pelvic tilt and hip extension during running. Comput Methods Biomech Biomed Engin 18:1926–1927. https://doi.org/10.1080/10255842.2015.1070582

Dewolf AH, Peñailillo LE, Willems PA (2016) The rebound of the body during uphill and downhill running at different speeds. J Exp Biol 219:2276–2288. https://doi.org/10.1242/jeb.142976

Dewolf AH, Ivanenko YP, Lacquaniti F, Willems PA (2017) Pendular energy transduction within the step during human walking on slopes at different speeds. PLoS ONE 12:e0186963. https://doi.org/10.1371/journal.pone.0186963

Dewolf AH, Ivanenko Y, Zelik KE et al (2018) Kinematic patterns while walking on a slope at different speeds. J Appl Physiol 125:642–653. https://doi.org/10.1152/japplphysiol.01020.2017

Dewolf AH, Ivanenko YP, Zelik KE et al (2019) Differential activation of lumbar and sacral motor pools during walking at different speeds and slopes. J Neurophysiol 122:872–887. https://doi.org/10.1152/jn.00167.2019

Dewolf AH, Ivanenko YP, Mesquita RM et al (2020a) Neuromechanical adjustments when walking with an aiding or hindering horizontal force. Eur J Appl Physiol 120:91–106. https://doi.org/10.1007/s00421-019-04251-1

Dewolf AH, Mesquita RM, Willems PA (2020b) Intra-limb and muscular coordination during walking on slopes. Eur J Appl Physiol. https://doi.org/10.1007/s00421-020-04415-4

Dewolf AH, Sylos-Labini F, Cappellini G et al (2020c) Emergence of different gaits in infancy: relationship between developing neural circuitries and changing biomechanics. Front Bioeng Biotechnol. https://doi.org/10.3389/fbioe.2020.00473

Dewolf AH, Sylos-Labini F, Cappellini G et al (2021a) Neuromuscular Age-related adjustment of gait when moving upwards and downwards. Front Hum Neurosci. https://doi.org/10.3389/fnhum.2021.749366

Dewolf AH, Sylos-Labini F, Cappellini G et al (2021b) Age-related changes in the neuromuscular control of forward and backward locomotion. PLoS ONE. https://doi.org/10.1371/journal.pone.0246372

Donelan JM, Kram R, Kuo AD (2002) Mechanical work for step-to-step transitions is a major determinant of the metabolic cost of human walking. J Exp Biol 205:3717–3727

Foster AD, Raichlen DA, Pontzer H (2013) Muscle force production during bent-knee, bent-hip walking in humans. J Hum Evol 65:294–302. https://doi.org/10.1016/j.jhevol.2013.06.012

Gebo DL (1992) Plantigrady and foot adaptation in African apes: Implications for hominid origins. Am J Phys Anthropol 89:29–58. https://doi.org/10.1002/ajpa.1330890105

Gill ML, Grahn PJ, Calvert JS et al (2018) Neuromodulation of lumbosacral spinal networks enables independent stepping after complete paraplegia. Nat Med 24:1677–1682. https://doi.org/10.1038/s41591-018-0175-7

Hallemans A, De Clercq D, Dongen SV, Aerts P (2006) Changes in foot-function parameters during the first 5 months after the onset of independent walking: a longitudinal follow-up study. Gait Posture 23:142–148. https://doi.org/10.1016/j.gaitpost.2005.01.003

Higurashi Y, Maier MA, Nakajima K et al (2019) Locomotor kinematics and EMG activity during quadrupedal versus bipedal gait in the Japanese macaque. J Neurophysiol 122:398–412. https://doi.org/10.1152/jn.00803.2018

Holowka NB, Lieberman DE (2018) Rethinking the evolution of the human foot: insights from experimental research. J Exp Bio. https://doi.org/10.1242/jeb.174425

Hu D, Xiong C-H, Sun R (2021) Working out the bipedal walking expenditure of energy based on foot morphology of different hominid genera: Implications for foot evolution. J Theoret Bio. https://doi.org/10.1016/j.jtbi.2021.110646

Huang T-WP, Shorter KA, Adamczyk PG, Kuo AD (2015) Mechanical and energetic consequences of reduced ankle plantar-flexion in human walking. J Exp Biol 218:3541–3550. https://doi.org/10.1242/jeb.113910

Ivanenko YP, Dominici N, Cappellini G et al (2004) Development of pendulum mechanism and kinematic coordination from the first unsupported steps in toddlers. J Exp Biol 207:3797–3810. https://doi.org/10.1242/jeb.01214

Ivanenko YP, Poppele RE, Lacquaniti F (2006) Spinal cord maps of spatiotemporal alpha-motoneuron activation in humans walking at different speeds. J Neurophysiol 95:602–618. https://doi.org/10.1152/jn.00767.2005

Ivanenko YP, Cappellini G, Poppele RE, Lacquaniti F (2008) Spatiotemporal organization of alpha-motoneuron activity in the human spinal cord during different gaits and gait transitions. Eur J Neurosci 27:3351–3368

Ivanenko YP, Dominici N, Cappellini G et al (2013) Changes in the spinal segmental motor output for stepping during development from infant to adult. J Neurosci 33:3025–3036a

Jessell T, Sürmeli G, Kelly J (2011) Motor neurons and the sense of place. Neuron 72:419–424. https://doi.org/10.1016/j.neuron.2011.10.021

Kendall F, McCreary E, Provance P et al (2005) Muscles. Testing and Function with Posture and Pain, Lippincott Williams and Wilkins, Baltimore

Kuliukas AV, Milne N, Fournier P (2009) The relative cost of bent-hip bent-knee walking is reduced in water. Homo 60:479–488. https://doi.org/10.1016/j.jchb.2009.09.002

La Scaleia V, Ivanenko YP, Zelik KE, Lacquaniti F (2014) Spinal motor outputs during step-to-step transitions of diverse human gaits. Front Hum Neurosci 8:305. https://doi.org/10.3389/fnhum.2014.00305

Lacquaniti F, Ivanenko YP, Zago M (2012) Patterned control of human locomotion. J Physiol (lond) 590:2189–2199. https://doi.org/10.1113/jphysiol.2011.215137

Lovejoy CO, McCollum MA (2010) Spinopelvic pathways to bipedality: why no hominids ever relied on a bent-hip–bent-knee gait. Phil Trans R Soc B 365:3289–3299. https://doi.org/10.1098/rstb.2010.0112

Martino G, Ivanenko YP, Serrao M et al (2014) Locomotor patterns in cerebellar ataxia. J Neurophysiol 112:2810–2821. https://doi.org/10.1152/jn.00275.2014

Mauroy G, Schepens B, Willems PA (2014) Leg stiffness and joint stiffness while running to and jumping over an obstacle. J Biomech 47:526–535. https://doi.org/10.1016/j.jbiomech.2013.10.039

Meurisse GM, Dierick F, Schepens B, Bastien GJ (2016) Determination of the vertical ground reaction forces acting upon individual limbs during healthy and clinical gait. Gait Posture 43:245–250. https://doi.org/10.1016/j.gaitpost.2015.10.005

Meurisse GM, Bastien GJ, Schepens B (2019) Effect of age and speed on the step-to-step transition phase during walking. J Biomech 83:253–259. https://doi.org/10.1016/j.jbiomech.2018.12.001

Monaco V, Rinaldi LA, Macrì G, Micera S (2009) During walking elders increase efforts at proximal joints and keep low kinetics at the ankle. Clin Biomech 24:493–498. https://doi.org/10.1016/j.clinbiomech.2009.04.004

Pontzer H (2007) Effective limb length and the scaling of locomotor cost in terrestrial animals. J Exp Biol 210:1752–1761. https://doi.org/10.1242/jeb.002246

Preuschoft H (1970) Mechanical analyses of primate feet - II. The foot as a whole. Z Anat Entwicklungsgesch 131:156–192. https://doi.org/10.1007/BF00523294

Santuz A, Brüll L, Ekizos A et al (2020) Neuromotor dynamics of human locomotion in challenging settings. Iscience 23(1):100796

Schmitt D, Larson SG (1995) Heel contact as a function of substrate type and speed in primates. Am J Phys Anthropol 96:39–50. https://doi.org/10.1002/ajpa.1330960105

Shapiro LJ, Jungers WL (1994) Electromyography of back muscles during quadrupedal and bipedal walking in primates. Am J Phys Anthropol 93:491–504. https://doi.org/10.1002/ajpa.1330930408

Stern JT Jr, Susman RL (1983) The locomotor anatomy of Australopithecus afarensis. Am J Phys Anthropol 60:279–317. https://doi.org/10.1002/ajpa.1330600302

Tomlinson BE, Irving D (1977) The numbers of limb motor neurons in the human lumbosacral cord throughout life. J Neurol Sci 34:213–219

Usherwood JR, Channon AJ, Myatt JP et al (2012) The human foot and heel-sole-toe walking strategy: a mechanism enabling an inverted pendular gait with low isometric muscle force? J R Soc Interface 9:2396–2402. https://doi.org/10.1098/rsif.2012.0179

Wang H, Li Y, Ning L (2014) Realization of a hydraulic actuated biped robot walking without double support phase. Int J Control Autom Syst 12:843–851. https://doi.org/10.1007/s12555-013-0257-8

Webber JT, Raichlen DA (2016) The role of plantigrady and heel-strike in the mechanics and energetics of human walking with implications for the evolution of the human foot. J Exp Biol 219:3729–3737. https://doi.org/10.1242/jeb.138610

Wei R-H, Zhao C, Rao J-S et al (2019) Neuromuscular control pattern in rhesus monkeys during bipedal walking. Exp Anim 68:341–349. https://doi.org/10.1538/expanim.18-0180